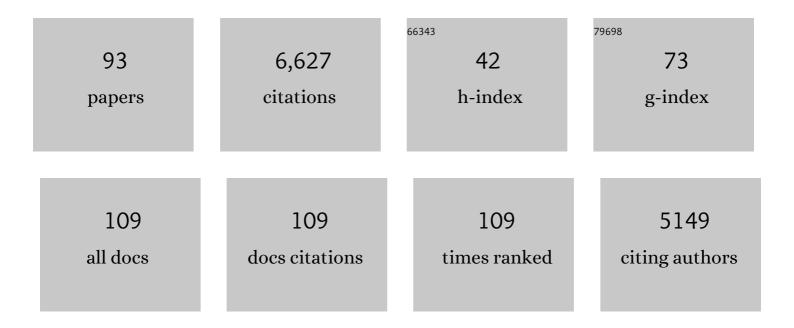
List of Publications by Year in descending order

Source: https://exaly.com/author-pdf/9168737/publications.pdf Version: 2024-02-01



#	Article	IF	CITATIONS
1	Mexico City aerosol analysis during MILAGRO using high resolution aerosol mass spectrometry at the urban supersite (T0) – Part 1: Fine particle composition and organic source apportionment. Atmospheric Chemistry and Physics, 2009, 9, 6633-6653.	4.9	525
2	An overview of the MILAGRO 2006 Campaign: Mexico City emissions and their transport and transformation. Atmospheric Chemistry and Physics, 2010, 10, 8697-8760.	4.9	349
3	Investigation of the sources and processing of organic aerosol over the Central Mexican Plateau from aircraft measurements during MILAGRO. Atmospheric Chemistry and Physics, 2010, 10, 5257-5280.	4.9	325
4	Emissions estimation from satellite retrievals: A review of current capability. Atmospheric Environment, 2013, 77, 1011-1042.	4.1	323
5	Air quality in North America's most populous city – overview of the MCMA-2003 campaign. Atmospheric Chemistry and Physics, 2007, 7, 2447-2473.	4.9	286
6	Measurement of ambient aerosols in northern Mexico City by single particle mass spectrometry. Atmospheric Chemistry and Physics, 2008, 8, 4499-4516.	4.9	257
7	A meteorological overview of the MILAGRO field campaigns. Atmospheric Chemistry and Physics, 2007, 7, 2233-2257.	4.9	199
8	Mexico city aerosol analysis during MILAGRO using high resolution aerosol mass spectrometry at the urban supersite (T0) – Part 2: Analysis of the biomass burning contribution and the non-fossil carbon fraction. Atmospheric Chemistry and Physics, 2010, 10, 5315-5341.	4.9	182
9	Distribution, magnitudes, reactivities, ratios and diurnal patterns of volatile organic compounds in the Valley of Mexico during the MCMA 2002 & 2003 field campaigns. Atmospheric Chemistry and Physics, 2007, 7, 329-353.	4.9	167
10	Correlation of secondary organic aerosol with odd oxygen in Mexico City. Geophysical Research Letters, 2008, 35, .	4.0	161
11	Characterizing ozone production in the Mexico City Metropolitan Area: a case study using a chemical transport model. Atmospheric Chemistry and Physics, 2007, 7, 1347-1366.	4.9	154
12	Black carbon over Mexico: the effect of atmospheric transport on mixing state, mass absorption cross-section, and BC/CO ratios. Atmospheric Chemistry and Physics, 2010, 10, 219-237.	4.9	140
13	Rapid ventilation of the Mexico City basin and regional fate of the urban plume. Atmospheric Chemistry and Physics, 2006, 6, 2321-2335.	4.9	130
14	Basin-scale wind transport during the MILAGRO field campaign and comparison to climatology using cluster analysis. Atmospheric Chemistry and Physics, 2008, 8, 1209-1224.	4.9	130
15	Satellite NO2 retrievals suggest China has exceeded its NOx reduction goals from the twelfth Five-Year Plan. Scientific Reports, 2016, 6, 35912.	3.3	126
16	Mexico City basin wind circulation during the MCMA-2003 field campaign. Atmospheric Chemistry and Physics, 2005, 5, 2267-2288.	4.9	124
17	Seasonal Variations of the Urban Heat Island at the Surface and the Near-Surface and Reductions due to Urban Vegetation in Mexico City. Journal of Applied Meteorology and Climatology, 2012, 51, 855-868.	1.5	113
18	Ozone Monitoring Instrument Observations of Interannual Increases in SO ₂ Emissions from Indian Coal-Fired Power Plants during 2005–2012. Environmental Science & Technology, 2013, 47, 13993-14000.	10.0	113

#	Article	IF	CITATIONS
19	Estimates of power plant NOx emissions and lifetimes from OMI NO2 satellite retrievals. Atmospheric Environment, 2015, 116, 1-11.	4.1	108
20	Enhanced Capabilities of TROPOMI NO ₂ : Estimating NO _{<i>X</i>} from North American Cities and Power Plants. Environmental Science & Technology, 2019, 53, 12594-12601.	10.0	103
21	The observed response of Ozone Monitoring Instrument (OMI) NO2 columns to NOx emission controls on power plants in the United States: 2005–2011. Atmospheric Environment, 2013, 81, 102-111.	4.1	99
22	Aerosol composition and source apportionment in the Mexico City Metropolitan Area with PIXE/PESA/STIM and multivariate analysis. Atmospheric Chemistry and Physics, 2006, 6, 4591-4600.	4.9	98
23	Hit from both sides: tracking industrial and volcanic plumes in Mexico City with surface measurements and OMI SO ₂ retrievals during the MILAGRO field campaign. Atmospheric Chemistry and Physics, 2009, 9, 9599-9617.	4.9	96
24	Emissions of nitrogen oxides from US urban areas: estimation from Ozone Monitoring Instrument retrievals for 2005–2014. Atmospheric Chemistry and Physics, 2015, 15, 10367-10383.	4.9	94
25	Relative impact of emissions controls and meteorology on air pollution mitigation associated with the Asia-Pacific Economic Cooperation (APEC) conference in Beijing, China. Science of the Total Environment, 2016, 571, 1467-1476.	8.0	83
26	Modelling constraints on the emission inventory and on vertical dispersion for CO and SO ₂ in the Mexico City Metropolitan Area using Solar FTIR and zenith sky UV spectroscopy. Atmospheric Chemistry and Physics, 2007, 7, 781-801.	4.9	82
27	In situ measurements of speciated atmospheric mercury and the identification of source regions in the Mexico City Metropolitan Area. Atmospheric Chemistry and Physics, 2009, 9, 207-220.	4.9	80
28	Model evaluation of methods for estimating surface emissions and chemical lifetimes from satellite data. Atmospheric Environment, 2014, 98, 66-77.	4.1	75
29	Ozone response to emission changes: a modeling study during the MCMA-2006/MILAGRO Campaign. Atmospheric Chemistry and Physics, 2010, 10, 3827-3846.	4.9	73
30	Impact of primary formaldehyde on air pollution in the Mexico City Metropolitan Area. Atmospheric Chemistry and Physics, 2009, 9, 2607-2618.	4.9	70
31	A top-down assessment using OMI NO ₂ suggests an underestimate in the NO _{<i>x</i>} emissions inventory in Seoul, South Korea, during KORUS-AQ. Atmospheric Chemistry and Physics, 2019. 19. 1801-1818.	4.9	68
32	Tula industrial complex (Mexico) emissions of SO ₂ and NO ₂ during the MCMA 2006 field campaign using a mobile mini-DOAS system. Atmospheric Chemistry and Physics, 2009, 9, 6351-6361.	4.9	63
33	Surface ozone at Nam Co in the inland Tibetan Plateau: variation, synthesis comparison and regional representativeness. Atmospheric Chemistry and Physics, 2017, 17, 11293-11311.	4.9	63
34	Composition and variation of noise recorded at the Yellowknife Seismic Array, 1991–2007. Journal of Geophysical Research, 2009, 114, .	3.3	59
35	Evaluation of WRF mesoscale simulations and particle trajectory analysis for the MILAGRO field campaign. Atmospheric Chemistry and Physics, 2009, 9, 4419-4438.	4.9	59
36	Distinct wind convergence patterns in the Mexico City basin due to the interaction of the gap winds with the synoptic flow. Atmospheric Chemistry and Physics, 2006, 6, 1249-1265.	4.9	58

#	Article	IF	CITATIONS
37	Seasonal Anisotropy in Short-Period Seismic Noise Recorded in South Asia. Bulletin of the Seismological Society of America, 2008, 98, 3033-3045.	2.3	57
38	Mobile mini-DOAS measurement of the outflow of NO ₂ and HCHO from Mexico City. Atmospheric Chemistry and Physics, 2009, 9, 5647-5653.	4.9	56
39	Characterizing ozone production and response under different meteorological conditions in Mexico City. Atmospheric Chemistry and Physics, 2008, 8, 7571-7581.	4.9	55
40	Gaseous and particulate pollutants in Lhasa, Tibet during 2013–2017: Spatial variability, temporal variations and implications. Environmental Pollution, 2019, 253, 68-77.	7.5	53
41	Satellite-derived land surface parameters for mesoscale modelling of the Mexico City basin. Atmospheric Chemistry and Physics, 2006, 6, 1315-1330.	4.9	51
42	Determination of particulate lead using aerosol mass spectrometry: MILAGRO/MCMA-2006 observations. Atmospheric Chemistry and Physics, 2010, 10, 5371-5389.	4.9	48
43	Positive association between short-term ambient air pollution exposure and children blood pressure in China–Result from the Seven Northeast Cities (SNEC) study. Environmental Pollution, 2017, 224, 698-705.	7.5	48
44	Using 3DVAR data assimilation system to improve ozone simulations in the Mexico City basin. Atmospheric Chemistry and Physics, 2008, 8, 7353-7366.	4.9	47
45	Quantitative estimation of meteorological impacts and the COVID-19 lockdown reductions on NO2 and PM2.5 over the Beijing area using Generalized Additive Models (GAM). Journal of Environmental Management, 2021, 291, 112676.	7.8	47
46	Impacts of control strategies, the Great Recession and weekday variations on NO 2 columns above North American cities. Atmospheric Environment, 2016, 138, 74-86.	4.1	44
47	Aerosol plume transport and transformation in high spectral resolution lidar measurements and WRF-Flexpart simulations during the MILAGRO Field Campaign. Atmospheric Chemistry and Physics, 2011, 11, 3543-3563.	4.9	43
48	Multi-year monitoring of atmospheric total gaseous mercury at a remote high-altitude site (Nam Co,) Tj ETQq0 0 10557-10574.	0 rgBT /O 4.9	verlock 10 Tf 42
49	Spatial and temporal variability of particulate polycyclic aromatic hydrocarbons in Mexico City. Atmospheric Chemistry and Physics, 2008, 8, 3093-3105.	4.9	40
50	Sources of nickel, vanadium and black carbon in aerosols in Milwaukee. Atmospheric Environment, 2012, 59, 294-301.	4.1	38
51	City-level variations in NOx emissions derived from hourly monitoring data in Chicago. Atmospheric Environment, 2018, 176, 128-139.	4.1	38
52	Changes in ozone photochemical regime in Fresno, California from 1994 to 2018 deduced from changes in the weekend effect. Environmental Pollution, 2020, 263, 114380.	7.5	34
53	Microseisms from Superstorm Sandy. Earth and Planetary Science Letters, 2014, 402, 324-336.	4.4	33
54	Competing PM2.5 and NO2 holiday effects in the Beijing area vary locally due to differences in residential coal burning and traffic patterns. Science of the Total Environment, 2021, 750, 141575.	8.0	32

#	Article	IF	CITATIONS
55	Developing intake fraction estimates with limited data: Comparison of methods in Mexico City. Atmospheric Environment, 2007, 41, 3672-3683.	4.1	29
56	First field-based atmospheric observation of the reduction of reactive mercury driven by sunlight. Atmospheric Environment, 2016, 134, 27-39.	4.1	28
57	Impact of regional transport on the anthropogenic and biogenic secondary organic aerosols in the Los Angeles Basin. Atmospheric Environment, 2015, 103, 171-179.	4.1	27
58	Long-range pollution transport during the MILAGRO-2006 campaign: a case study of a major Mexico City outflow event using free-floating altitude-controlled balloons. Atmospheric Chemistry and Physics, 2010, 10, 7137-7159.	4.9	25
59	Estimating sources of elemental and organic carbon and their temporal emission patterns using a least squares inverse model and hourly measurements from the St. Louis–Midwest supersite. Atmospheric Chemistry and Physics, 2015, 15, 2405-2427.	4.9	25
60	First measurement of atmospheric mercury species in Qomolangma Natural Nature Preserve, Tibetan Plateau, and evidence oftransboundary pollutant invasion. Atmospheric Chemistry and Physics, 2019, 19, 1373-1391.	4.9	23
61	A global perspective on national climate mitigation priorities in the context of air pollution and sustainable development. City and Environment Interactions, 2019, 1, 100003.	4.2	22
62	Identification of potential source areas for elevated PM2.5, nitrate and sulfate concentrations. Atmospheric Environment, 2013, 71, 187-197.	4.1	21
63	Source apportionment of PM2.5 organic carbon in the San Joaquin Valley using monthly and daily observations and meteorological clustering. Environmental Pollution, 2018, 237, 366-376.	7.5	21
64	Impacts of regional transport on black carbon in Huairou, Beijing, China. Environmental Pollution, 2017, 221, 75-84.	7.5	20
65	Estimation of mercury emissions from forest fires, lakes, regional and local sources using measurements in Milwaukee and an inverse method. Atmospheric Chemistry and Physics, 2012, 12, 8993-9011.	4.9	19
66	Assessment of forest fire impacts on carbonaceous aerosols using complementary molecular marker receptor models at two urban locations in California's San Joaquin Valley. Environmental Pollution, 2019, 246, 274-283.	7.5	19
67	An improved understanding of NOx emissions in South Asian megacities using TROPOMI NO ₂ retrievals. Environmental Research Letters, 2022, 17, 024006.	5.2	19
68	The oxidative potential and biological effects induced by PM10 obtained in Mexico City and at a receptor site during the MILAGRO Campaign. Environmental Pollution, 2011, 159, 3446-3454.	7.5	17
69	Estimation of direct emissions and atmospheric processing of reactive mercury using inverse modeling. Atmospheric Environment, 2014, 85, 73-82.	4.1	17
70	Influence of transboundary air pollution on air quality in southwestern China. Geoscience Frontiers, 2021, 12, 101239.	8.4	17
71	Modeling Inorganic Aerosols and Their Response to Changes in Precursor Concentration in Mexico City. Journal of the Air and Waste Management Association, 2005, 55, 803-815.	1.9	15
72	Origin of high particle number concentrations reaching the St. Louis, Midwest Supersite. Journal of Environmental Sciences, 2015, 34, 219-231.	6.1	14

#	Article	IF	CITATIONS
73	Latest observations of total gaseous mercury in a megacity (Lanzhou) in northwest China. Science of the Total Environment, 2020, 720, 137494.	8.0	14
74	Unstructured pressure-correction solver based on a consistent discretization of the Poisson equation. International Journal for Numerical Methods in Fluids, 2000, 34, 463-478.	1.6	13
75	Sources of metals and bromine-containing particles in Milwaukee. Atmospheric Environment, 2013, 73, 124-130.	4.1	13
76	Evaluation of Stratospheric Intrusions and Biomass Burning Plumes on the Vertical Distribution of Tropospheric Ozone Over the Midwestern United States. Journal of Geophysical Research D: Atmospheres, 2020, 125, e2020JD032454.	3.3	13
77	Improved PM _{2.5} concentration estimates from low-cost sensors using calibration models categorized by relative humidity. Aerosol Science and Technology, 2021, 55, 600-613.	3.1	13
78	Impacts of Indian summer monsoon and stratospheric intrusion on air pollutants in the inland Tibetan Plateau. Geoscience Frontiers, 2021, 12, 101255.	8.4	13
79	Modeling ultrafine particle growth at a pine forest site influenced by anthropogenic pollution during BEACHON-RoMBAS 2011. Atmospheric Chemistry and Physics, 2014, 14, 11011-11029.	4.9	12
80	A hybrid method for PM2.5 source apportionment through WRF-Chem simulations and an assessment of emission-reduction measures in western China. Atmospheric Research, 2020, 236, 104787.	4.1	12
81	Changes in speciated PM2.5 concentrations in Fresno, California, due to NOx reductions and variations in diurnal emission profiles by day of week. Elementa, 2019, 7, .	3.2	12
82	Contributions of wood smoke and vehicle emissions to ambient concentrations of volatile organic compounds and particulate matter during the Yakima wintertime nitrate study. Journal of Geophysical Research D: Atmospheres, 2017, 122, 1871-1883.	3.3	11
83	Source attribution of black and Brown carbon near-UV light absorption in Beijing, China and the impact of regional air-mass transport. Science of the Total Environment, 2022, 807, 150871.	8.0	11
84	Impacts of secondary aerosol formation and long range transport on severe haze during the winter of 2017 in the Seoul metropolitan area. Science of the Total Environment, 2022, 804, 149984.	8.0	10
85	Distinguishing Air Pollution Due to Stagnation, Local Emissions, and Long-Range Transport Using a Generalized Additive Model to Analyze Hourly Monitoring Data. ACS Earth and Space Chemistry, 2021, 5, 2329-2340.	2.7	8
86	First observation of mercury species on an important water vapor channel in the southeastern Tibetan Plateau. Atmospheric Chemistry and Physics, 2022, 22, 2651-2668.	4.9	8
87	Impacts of Sources on PM _{2.5} Oxidation Potential during and after the Asia-Pacific Economic Cooperation Conference in Huairou, Beijing. Environmental Science & Technology, 2020, 54, 2585-2594.	10.0	6
88	Source attribution of air pollution using a generalized additive model and particle trajectory clusters. Science of the Total Environment, 2021, 780, 146458.	8.0	6
89	The investigations on organic sources and inorganic formation processes and their implications on haze during late winter in Seoul, Korea. Environmental Research, 2022, 212, 113174.	7.5	5
90	A potential route for photolytic reduction of HgCl2 and HgBr2 in dry air and analysis about the impacts from Ozone. Atmospheric Research, 2021, 249, 105310.	4.1	4

#	Article	IF	CITATIONS
91	Chemical speciation of PM2.5 in Tehran: Quantification of dust contribution and model validation. Atmospheric Pollution Research, 2020, 11, 1839-1846.	3.8	2
92	The design of improved smoothing operators for finite volume flow solvers on unstructured meshes. International Journal for Numerical Methods in Fluids, 2001, 36, 903-923.	1.6	1
93	"Military Parade Blue Skies―in Beijing: Decisive Influence of Meteorological Factors on Transport Channel and Atmospheric Pollutant Concentration Level. Atmosphere, 2021, 12, 636.	2.3	1